

Hole-doping evolution of the quasiparticle band in models of strongly correlated electrons for the high- T_c cuprates

Daniel Duffy

Department of Physics and National High Magnetic Field Lab, Florida State University, Tallahassee, Florida 32306

Alexander Nazarenko

Department of Physics, Boston College, Chestnut Hill, Massachusetts 02167

Stephan Haas

Theoretische Physik, Eidgenössische Technische Hochschule, 8093 Zürich, Switzerland

Adriana Moreo

Department of Physics and National High Magnetic Field Lab, Florida State University, Tallahassee, Florida 32306

Jose Riera

Instituto de Fisica Rosario, Avenida 27 de Febrero 210 bis, 2000 Rosario, Argentina

Elbio Dagotto

Department of Physics and National High Magnetic Field Lab, Florida State University, Tallahassee, Florida 32306

(Received 7 January 1997; revised manuscript received 3 March 1997)

Quantum Monte Carlo (QMC) and maximum-entropy techniques are used to study the spectral function $A(\mathbf{p}, \omega)$ of the one-band Hubbard model with strong coupling including a next-nearest-neighbor electronic hopping with amplitude $t'/t = -0.35$. These values of parameters are chosen to improve the comparison of the Hubbard model with angle-resolved photoemission (ARPES) data for $\text{Sr}_2\text{CuO}_2\text{Cl}_2$. A narrow quasiparticle (qp) band is observed in the QMC analysis at the temperature of the simulation $T = t/3$, both at and away from half-filling. Such a narrow band produces a large accumulation of weight in the density of states at the top of the valence band. As the electronic density $\langle n \rangle$ decreases further away from half-filling, the chemical potential travels through this energy window with a large number of states, and by $\langle n \rangle \sim 0.70$ it has crossed it entirely. The region near momentum $(0, \pi)$ and $(\pi, 0)$ in the spectral function is more sensitive to doping than momenta along the diagonal from $(0, 0)$ to (π, π) . The evolution with hole density of the quasiparticle dispersion contains some of the features observed in recent ARPES data in the underdoped regime. For sufficiently large hole densities the “flat” bands at $(\pi, 0)$ cross the Fermi energy, a prediction that could be tested with ARPES techniques applied to overdoped cuprates. The population of the qp band introduces a *hidden* density in the system which produces interesting consequences when the quasiparticles are assumed to interact through antiferromagnetic fluctuations and studied with the BCS gap-equation formalism. In particular, a region of extended *s*-wave character is found to compete with the *d* wave in the overdoped regime, i.e., when the chemical potential has almost entirely crossed the qp band as $\langle n \rangle$ is reduced. The present study also shows that previous “real-space” pairing theories for the cuprates, such as the antiferromagnetic Van Hove scenario, originally constructed based on information gathered at half-filling, do not change their predictions if hole dispersions resembling noninteracting electrons with renormalized parameters are used.

[S0163-1829(97)00433-5]

I. INTRODUCTION

Recent studies of $\text{Bi}_2\text{Sr}_2\text{Ca}_{1-x}\text{Dy}_x\text{Cu}_2\text{O}_{8+\delta}$ using angle-resolved photoemission (ARPES) techniques have provided the evolution of the quasiparticle band as the hole density changes in the underdoped regime of the high- T_c cuprates.¹⁻³ These studies complement previous ARPES analysis of the hole dispersion in the antiferromagnetic insulator $\text{Sr}_2\text{CuO}_2\text{Cl}_2$.^{4,5} The overall results emerging from these experiments can be summarized as follows: (i) the bandwidth of the quasiparticle band is a fraction of eV, i.e., narrower than generally predicted by band-structure calculations. This result suggests that strong correlations are

important in the generation of the quasiparticle dispersion; (ii) the two-dimensional (2D) *t*-*J* model explains accurately the bandwidth for a hole injected in the insulator, as well as the details of the dispersion along the main diagonal in momentum space from $\mathbf{p} = (0, 0)$ to (π, π) (in the 2D square lattice notation);⁴ (iii) however, the behavior along the direction from $(0, \pi)$ to $(\pi, 0)$ is not properly described by the *t*-*J* model which predicts a near degeneracy between momenta along this line,⁶ in contradiction with experiments. The ARPES data for the antiferromagnetic insulator show that the quasiparticle signal at $(\pi, 0)$ is very weak, and about 0.3 eV deeper in energy than $(\pi/2, \pi/2)$;⁴ (iv) as the density of holes grows the region near $(\pi, 0)$ moves towards the

chemical potential which is approximately reached at the optimal concentration,¹ while the main diagonal $(0,0) - (\pi, \pi)$ is less affected; (v) at optimal doping remarkably “flat” bands at $(\pi, 0)$ near the Fermi energy have been observed.⁷

The results of Marshall *et al.*¹ have been interpreted as providing evidence for “hole pockets” in the underdoped regime caused by short-distance antiferromagnetic correlations, although other explanations such as preformed pairs are also possible.^{8,9} As explained before, the standard t - J model is not enough to provide all the details of the ARPES results at half-filling, and thus presumably it cannot explain the data away from half-filling either. However, the t - J model is just one possible Hamiltonian to describe the behavior of holes in an antiferromagnetic background. While the model is attractive for its simplicity, there is no symmetry or renormalizability argument signaling it as unique for the description of the cuprates. For this reason Nazarenko *et al.*¹⁰ recently introduced extra terms in the t - J Hamiltonian to improve the agreement with experiments. Adding an electronic hopping along the diagonals of the elementary plaquettes (with amplitude $t'/t = -0.35$) the results for the insulator were improved since the position of the quasiparticle (qp) at $(\pi, 0)$ proved to be very sensitive to the strength of extra hole hopping terms in the model. Actually, the qp peak at this momentum moves towards larger binding energies as a negative t'/t grows in amplitude.¹⁰ This idea has been used by several other groups which, in addition to hoppings along the plaquette diagonals, have included hoppings at distance of two lattice spacings with amplitude t'' to obtain an even better agreement with experiments.¹¹

The purpose of this paper is to report on results for the density dependence of the quasiparticle dispersion corresponding to the one-band Hubbard model with a next-nearest-neighbor hopping t' working in the strong Coulomb coupling regime. It is expected that the U - t - t' and t - t' - J models produce qualitatively similar physics at large U/t . As a numerical technique we use the quantum Monte Carlo method supplemented by maximum-entropy analysis. The success of the t - t' - J model at half-filling^{10,11} and the recent availability of ARPES data in the underdoped regime¹⁻³ prompted us to carry out this study. Note that although the numerical methods used here are powerful, their accuracy is limited and, thus, our results are mostly qualitative rather than quantitative. Nevertheless, from the analysis of the present QMC data and also comparing our results against those produced previously for the t - J and Hubbard models here we arrive to the conclusion that at least some features of the experimental ARPES evolution of the hole dispersion can be explained using one-band electronic models. Experimental predictions are made to test the calculations. The presence of a narrow quasiparticle band in the spectrum and its crossing by the chemical potential as the electronic density is reduced are key features for the discussions below.

The present paper is not only devoted to the analysis of QMC results and its comparison with ARPES data, but it also addresses the influence of hole doping in recently proposed theories for the cuprates.¹² In these theories the hole dispersion is calculated at half-filling and assumed to change only slightly as the hole density grows. Hole attraction is assumed to be dominated by the minimization of antiferro-

magnetic (AF) broken bonds, which implies the presence of an effective nearest-neighbor (NN) density-density attraction proportional to the exchange J . Superconductivity in the $d_{x^2-y^2}$ channel is natural in this scenario¹² due to the strong AF correlations.^{6,13} The interaction of holes is better visualized in *real space*, i.e., with pairing occurring when dressed holes share a spin polaronic cloud, as in the spin-bag mechanism.¹⁴ This real-space picture (see also Ref. 15) holds even for a small AF correlation length, ξ_{AF} , and in this scenario there is no need to tune parameters to work very close to an AF instability as in other approaches.

To obtain quantitative information from these intuitive ideas, holes moving with a dispersion calculated using one hole in an AF background, $\epsilon_{AF}(\mathbf{p})$, and interacting through the NN attractive potential mentioned before, have been previously analyzed.¹² Within a rigid band filling of $\epsilon_{AF}(\mathbf{p})$ and using a BCS formalism, $d_{x^2-y^2}$ superconductivity dominates with $T_c \sim 100$ K caused by a large density of states (DOS) that appears in the hole dispersion. The idea has many similarities with previous scenarios that used van Hove (vH) singularities in the band structure to increase T_c ,¹⁶ although d -wave superconductivity is not natural in this context unless AF correlations are included. However, the rigid band filling is an approximation whose accuracy remains to be tested. In particular, the following questions naturally arise: (i) does the qp peak in the DOS found at $\langle n \rangle = 1$ survive a finite hole density; (ii) to what extent do the changes in the qp dispersion with doping affect previous calculations in this framework; (iii) are the “shadow” regions generated by AF correlations^{14,17-19} important for real-space pairing approaches? With the help of the present QMC results, as well as previous simulations, in this paper all these issues are discussed. The overall conclusion is that as long as the hole density is such that the ξ_{AF} is at least of a couple of lattice spacings, the predictions of previous scenarios¹² and other similar theories remain qualitatively the same, in spite of substantial changes occurring in the hole dispersion with doping.

The organization of the paper is as follows: in Sec. II the model and details of the numerical method are discussed. Section III contains the QMC-ME results both at half-filling and with a finite hole density. In Sec. IV the results are discussed and compared with ARPES experiments. Implications for real-space theories of high T_c are extensively studied in Sec. V. Results of previous publications are also used to construct a simple picture for the behavior of electrons in the Hubbard model. Section VI contains a summary of the paper and its experimental predictions.

II. MODEL AND NUMERICAL TECHNIQUE

The one-band Hubbard Hamiltonian with next-nearest-neighbor hopping is given by

$$H = -t \sum_{\langle \mathbf{ij} \rangle, \sigma} (c_{\mathbf{i}, \sigma}^\dagger c_{\mathbf{j}, \sigma} + \text{H.c.}) - t' \sum_{\langle\langle \mathbf{ij} \rangle\rangle, \sigma} (c_{\mathbf{i}, \sigma}^\dagger c_{\mathbf{j}, \sigma} + \text{H.c.}) + U \sum_{\mathbf{i}} (n_{\uparrow\mathbf{i}} - 1/2)(n_{\downarrow\mathbf{i}} - 1/2) + \mu \sum_{\mathbf{i}, \sigma} n_{\mathbf{i}\sigma}, \quad (1)$$

where $c_{\mathbf{i}, \sigma}^\dagger$ creates an electron at site \mathbf{i} with spin projection σ , $n_{\mathbf{i}\sigma}$ is the number operator, the sum $\langle\langle \mathbf{ij} \rangle\rangle$ runs over pairs of

nearest-neighbor lattice sites, $\langle\langle\mathbf{ij}\rangle\rangle$ runs over pairs of lattice sites along the plaquette diagonals, U is the on-site Coulombic repulsion, t the nearest-neighbor hopping amplitude, t' is the plaquette diagonal hopping amplitude, and μ the chemical potential. Throughout this study we will set $t=1$, $t'/t=-0.35$, and use periodic boundary conditions.

Using standard QMC methods,²⁰ we have obtained the imaginary-time Green's functions at finite temperature. The method of maximum entropy²¹ was used to analytically continue the imaginary-time Green's functions to obtain the spectral weight function $A(\mathbf{p},\omega)$. Previous studies using this method have concentrated on, e.g., the one-dimensional²² and two-dimensional Hubbard model at and away from half-filling.^{18,23-25} However, with the next-nearest-neighbor hopping term only a few results have been obtained with this technique²⁶ since the additional hopping amplitude exacerbates the sign problem (which exists even at half-filling).

In this paper, we present a systematic study of the evolution of the spectral function in the U - t - t' model at electronic densities ranging from half-filling ($\langle n \rangle = 1.0$) to quarter-filling ($\langle n \rangle = 0.5$) on a 6×6 lattice at an inverse temperature of $\beta t = 3$ ($T = 0.33t$). The procedure we used to obtain these results is slightly different from those used before,^{25,26} and we believe that it provides more details to the spectral function. First, approximately 100 000 QMC measurement sweeps were taken at each density (for a fixed T , t'/t , and U/t) to obtain accurate statistics for the imaginary-time Green's functions. Once the spectral function was obtained from the standard ME procedure, we used this spectral function as a seed for further ME analysis with a reduced coefficient of the entropy α .^{21,27}

In order to work in the realistic strong-coupling regime, sacrifices in the lattice size and temperature had to be made due to the sign problem.²⁸ The same set of measurements shown below in Sec. III could have been performed on an 8×8 lattice. However, it would have required a higher temperature ($\beta t = 2$) to obtain good statistics on the imaginary-time Green's functions thereby washing out parts of the quasiparticle features that become prominent at lower temperatures. Since at half-filling and $\beta t = 2$, the 6×6 and 8×8 lattices give qualitatively similar results and we were able to reach a lower temperature using the smaller lattice, then we decided to use the 6×6 cluster throughout the paper.

III. QMC RESULTS

A. Half-filling

In Fig. 1, the QMC results obtained at half-filling for $U=10t$, $T=t/3$, and $t'/t=-0.35$ are shown. Figure 1(a) contains $A(\mathbf{p},\omega)$ after the ME analysis of the QMC data. The asymmetry of most of the dominant peaks suggests that they are a combination of at least two features located at different energies. This is reasonable since previous calculations for the U - t model (see, e.g., Ref. 25) have established that below the chemical potential $A(\mathbf{p},\omega)$ is made out of a quasiparticle (qp) peak near μ , carrying a small fraction of the total weight, and a broad incoherent (INC) feature at larger binding energies containing the rest of the weight. $A(\mathbf{p},\omega)$ have been fitted by two Gaussians with positions, widths, and

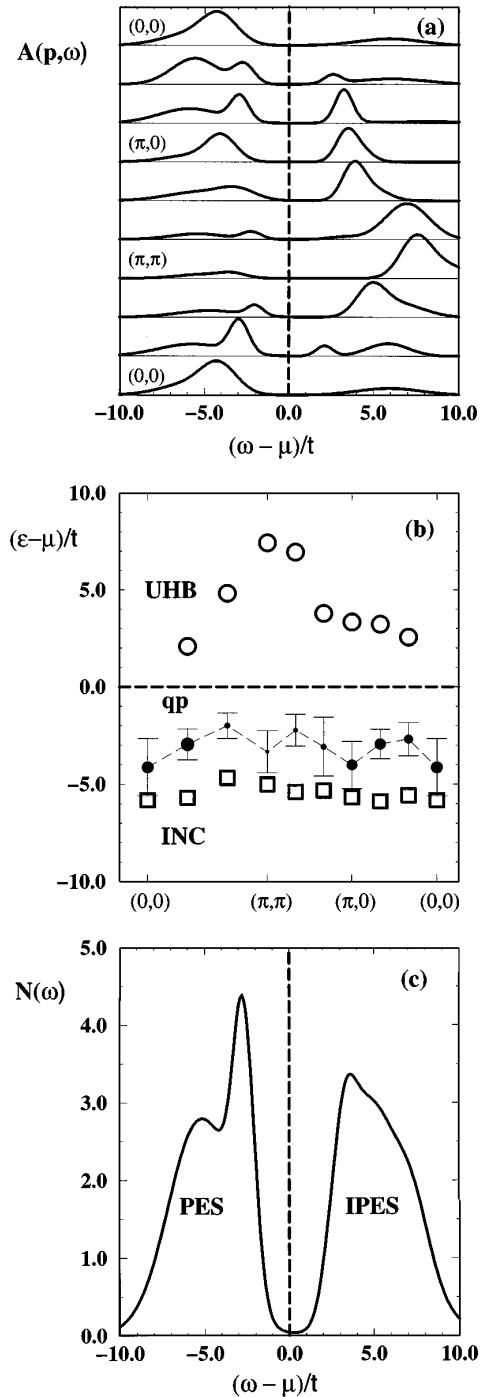


FIG. 1. (a) Spectral functions $A(\mathbf{p},\omega)$ of the U - t - t' Hubbard model at $U/t=10$, $t'/t=-0.35$, and $T=t/3$, using QMC-ME techniques on a 6×6 cluster. The density is $\langle n \rangle = 1.0$. From the bottom, the momenta are along the main diagonal from $(0,0)$ to (π,π) , from there to $(\pi,0)$, and finally back to $(0,0)$; (b) energies of the dominant peaks in the spectral functions. The results in the PES region are obtained from a two-Gaussian analysis of the QMC-ME results. The squares correspond to the incoherent part of the spectrum (INC) and its error bars are not shown. The full circles form the quasiparticle (qp) band, and their diameter is proportional to the intensity. The error bars are given by the width at half the height of the Gaussian corresponding to the qp peak at each momenta. The upper Hubbard band is also shown (open circles) without error bars; (c) density of states $N(\omega)$ obtained by summing the $A(\mathbf{p},\omega)$'s.

weights adjusted to match the ME result, keeping the overall weight constant. The same study was performed above the chemical potential in the inverse photoemission (IPES) regime but such analysis did not provide interesting information since the weight of the peak the closest to μ is very small, especially away from half-filling. Then, within the accuracy of the present QMC-ME study, the upper Hubbard band is described as just containing a broad featureless peak for each momentum. The two-peak decomposition analysis reported here will, thus, be limited to the PES part of the spectrum. However, note that at least at half-filling it is likely that the IPES portion of the spectrum contains a (low intensity) qp-like feature. In particular, as $t'/t \rightarrow 0$ particle-hole symmetry must be recovered, and here the peaks appearing in the PES region must also exist in the IPES regime. Nevertheless, in Sec. III B below we will show that at finite hole densities the qp band at the bottom of the UHB carries such a small weight that it can be neglected.

Following this fitting procedure, in Fig. 1(b) the energy position of the peaks as a function of momentum is shown. As anticipated, below μ a feature at the top of the valence band appears. It is natural to associate this peak with a ‘‘quasiparticle band.’’ The bandwidth is roughly $2t$, i.e., much smaller than for free electrons on a lattice. However, it is not as small as predicted by t - J model calculations,⁶ which may be due to the influence of t' or a finite U/t . The top of the qp band is located along the main diagonal from $(0,0)$ to (π, π) , in agreement with previous literature.⁶ The influence of the nonzero next-nearest-neighbor (NNN) hopping t' appears in the energy position of the qp band at $(\pi, 0)$ which is deeper in energy than $(2\pi/3, 2\pi/3)$ and $(\pi/3, \pi/3)$ [while for $t'/t=0.0$, $(\pi, 0)$ is located very close to the top of the band in contradiction with ARPES experiments for cuprate insulators⁴]. It is likely that on larger clusters $(\pi/2, \pi/2)$ would correspond to the actual top of the qp band, as predicted before.⁶ The overall shape of the qp band is similar to that calculated in the t - J model using the self-consistent Born approximation.¹⁰

It is interesting to note that the qp band includes momentum (π, π) , although with a very small intensity. This is reasonable for two reasons: (i) first, the presence of a charge gap in the spectrum, as clearly seen in Fig. 1(b), suggests that bands starting, say, at $(0,0)$ cannot simply disappear at some other momentum by crossing μ . By continuity they have to extend all along the Brillouin zone (unless their qp weight vanishes); (ii) in addition, the presence of strong antiferromagnetic correlations implies a doubling of the unit cell of dynamical origin and thus ‘‘shadow band’’ features should appear in the spectrum, as discussed in several models with strong antiferromagnetic correlations.^{14,17–19,24,30,29,31} In other words, AF introduces an extra symmetry in the problem that links \mathbf{p} with $\mathbf{p}+(\pi, \pi)$. These shadow features are certainly weak compared to the rest of the band, but are nevertheless present in the spectrum of Fig. 1(b).

The rest of the spectral weight is contained in the broad incoherent feature at energies deeper than the qp peak, and also in the upper Hubbard band (UHB). The latter presents some nontrivial momentum dependence near (π, π) . This behavior seems a remnant of the results for noninteracting electrons. Finally, Fig. 1(c) contains the density of states

(DOS) $N(\omega) = \sum_{\mathbf{p}} A(\mathbf{p}, \omega)$ at half-filling. The gap $\Delta \sim 5t$ and the sharp qp band can be clearly identified.

B. Finite hole density

Figure 2 contains the QMC-ME results obtained at density $\langle n \rangle = 0.94$, with the rest of the parameters as in Fig. 1. In Fig. 2(a) the spectral weight $A(\mathbf{p}, \omega)$ is shown. There are several interesting features in this result. For example, the upper Hubbard band has lost weight compared with results at $\langle n \rangle = 1.0$. This is not surprising since as the hole density grows the chances that an electron injected in the lattice will populate already occupied sites is reduced.

The most interesting physical consequences of hole doping are obtained in the PES region. Here the chemical potential has moved to the top of the valence band, more specifically into the qp band. Figure 2(b) shows the results of a two-peak analysis of the PES region similar to that performed at half-filling. Interpolating results along the main diagonal, it is observed that the qp peak at momentum $\mathbf{p}=(\pi/2, \pi/2)$ should be approximately at the chemical potential for this density, while $(\pi, 0)$ is still about $2t$ below. The qp band has distorted its shape in such a way that considerable weight has been moved above μ in the vicinity of (π, π) . Actually, now the qp band resembles a more standard tight-binding dispersion although with a renormalized hopping amplitude smaller than the bare one. Note, however, that the position of the qp peak at momentum $(0,0)$ is somewhat pathological since it is located above the chemical potential. We do not have an explanation for this anomalous behavior, which likely is caused by the maximum entropy procedure. The incoherent part of the spectrum is also clearly visible in the calculation. At this density it remains entirely filled, i.e., the electrons removed from the system have been taken from the qp band. Finally, note that the shadow features are no longer prominent. This is correlated with a substantial reduction of the antiferromagnetic correlation length ξ_{AF} at this density and temperature compared with the results at half-filling. This is not in contradiction with claims that recently observed features in ARPES are induced by antiferromagnetism^{17,18} since at very low temperatures ξ_{AF} likely remains robust for a larger hole density region near half-filling than it occurs at the relatively high temperature $T=t/3$. In Fig. 2(c), the DOS for $\langle n \rangle = 0.94$ is shown. The qp band is sharp, and μ lies slightly to the right of the top of this band [see inset of Fig. 2(c)]. A pseudogap generated by the large coupling U/t is still clearly visible.

Figure 3(a) contains the QMC-ME results obtained at $\langle n \rangle = 0.84$. Compared with the results at $\langle n \rangle = 0.94$, now μ is located deeper inside the qp band according to the two-Gaussian analysis presented in Fig. 3(b). Interpolations clearly show that $\mathbf{p}=(\pi/2, \pi/2)$ for this band is now in the IPES region, while $(\pi, 0)$ is at or very close to μ but still in the PES regime. The incoherent weight in PES remains robust. Figure 3(c) shows the DOS at this density. μ is located slightly to the left of the qp band maximum, the pseudogap has virtually melted, and there is only a tiny trace of the upper Hubbard band. The presence of $(\pi, 0)$ very close to μ is correlated with experimental results showing ‘‘flat bands’’ near the Fermi energy at optimal doping.^{7,32,30,33}

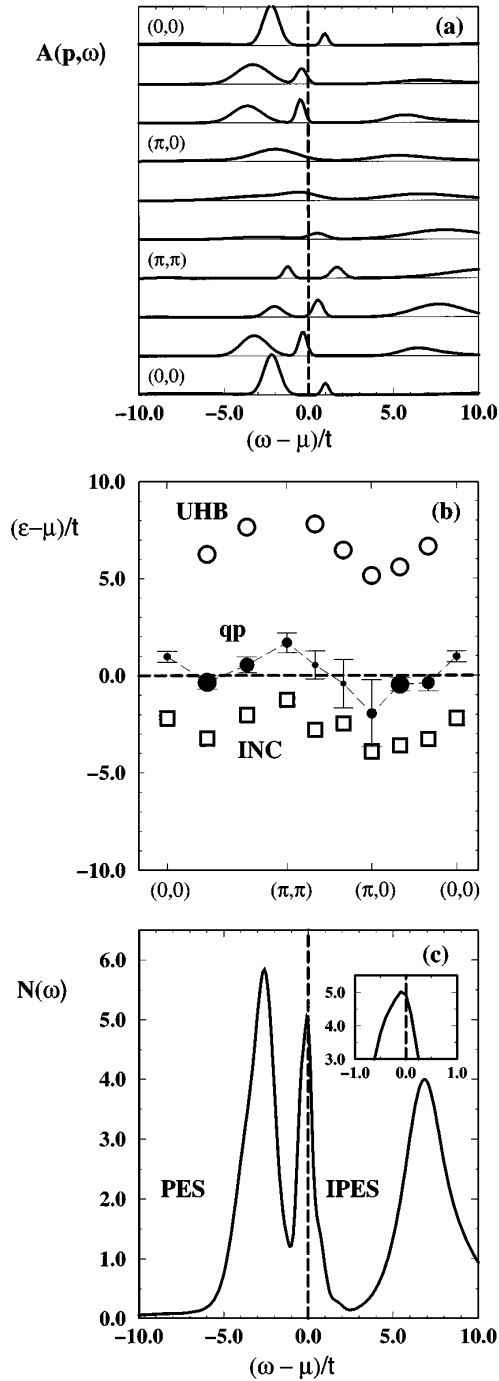


FIG. 2. (a) Spectral functions $A(\mathbf{p}, \omega)$ of the U - t - t' Hubbard model at $U/t=10$, $t'/t=-0.35$, and $T=t/3$, using QMC-ME techniques on a 6×6 cluster. The density is $\langle n \rangle = 0.94$. From the bottom, the momenta are along the main diagonal from $(0,0)$ to (π, π) , from there to $(\pi,0)$, and finally back to $(0,0)$; (b) energies of the dominant peaks in the spectral functions. The results in the PES region are obtained from a two-Gaussian analysis of the QMC-ME results. The squares correspond to the incoherent part of the spectrum (INC) and its error bars are not shown. The full circles form the quasiparticle (qp) band, and their diameter is proportional to the intensity. The error bars are given by the width at half the height of the Gaussian corresponding to the qp peak at each momenta. The upper Hubbard band is also shown (open circles) without error bars; (c) density of states $N(\omega)$ obtained by summing the $A(\mathbf{p}, \omega)$'s. The inset shows the top of the qp peak in more detail.

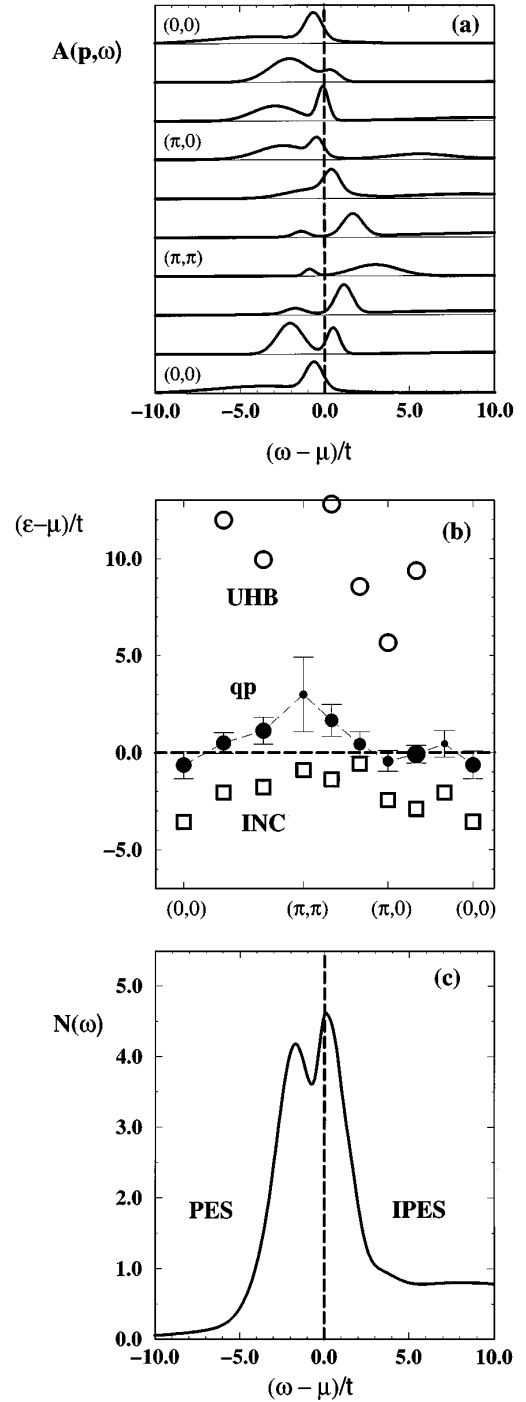


FIG. 3. (a) Spectral functions $A(\mathbf{p}, \omega)$ of the U - t - t' Hubbard model at $U/t=10$, $t'/t=-0.35$, and $T=t/3$, using QMC-ME techniques on a 6×6 cluster. The density is $\langle n \rangle = 0.84$. From the bottom, the momenta are along the main diagonal from $(0,0)$ to (π, π) , from there to $(\pi,0)$, and finally back to $(0,0)$; (b) energies of the dominant peaks in the spectral functions. The results in the PES region are obtained from a two-Gaussian analysis of the QMC-ME results. The squares correspond to the incoherent part of the spectrum (INC) and its error bars are not shown. The full circles form the quasiparticle (qp) band, and their diameter is proportional to the intensity. The error bars are given by the width at half the height of the Gaussian corresponding to the qp peak at each momenta. The upper Hubbard band is also shown (open circles) without error bars; (c) density of states $N(\omega)$ obtained by summing the $A(\mathbf{p}, \omega)$'s.

Figure 4 contains the QMC results obtained at $\langle n \rangle = 0.78$. This density is particularly interesting since now μ seems to have crossed most of the qp band.³⁴ This can be observed directly in the spectral weight [Fig. 4(a)], and in its two-peak analyzed output [Fig. 4(b)]. This detail will have interesting consequences for some theories of high- T_c cuprates, as described later in this paper. The DOS is shown in Fig. 4(c). The same trend is also observed at $\langle n \rangle = 0.65$ for which here only the DOS is shown (Fig. 5). At this density the qp band is empty, and the INC feature becomes sharper presumably due to its proximity to the chemical potential. It is interesting to note that the chemical potential in Fig. 5 is located at a sharp minimum in the density of states.

Results at $\langle n \rangle = 0.47$ (Fig. 6) show that the qp band has melted, and at this low density, the spectral weight is dominated by features that can be traced back to the incoherent part of the PES spectrum at half-filling [Fig. 6(a)]. In Fig. 6(b) the position of the dominant peak is given as a function of momentum, and in Fig. 6(c) the DOS is shown. It is interesting that now the results are nicely fitted by the noninteracting tight-binding dispersion [solid line in Fig. 6(b)]. Thus, the ‘‘free-electron’’ limit is approximately recovered in the strong-coupling regime at ‘‘quarter-filling.’’ Again, note that the peak structure in the spectrum seems to have emerged from the incoherent part of the valence band observed at half-filling.

IV. COMPARISON OF QMC-ME RESULTS WITH ARPES EXPERIMENTS

As discussed in the Introduction, ARPES results have shown that the quasiparticle peak at $\mathbf{p} = (\pi, 0)$ is very sensitive to hole doping at least in the underdoped regime.^{1,2} For the same densities, the qp dispersion along the main diagonal from $(0, 0)$ to (π, π) does not change as much. In this section it will be investigated if the numerical results of Sec. III are compatible with the ARPES data.

In Fig. 7, we schematically show what occurs upon doping when a tight-binding dispersion including a NN hopping amplitude t^* , and a NNN amplitude t'^* with a ratio $t'^*/t^* = -0.35$ is used. The reason for this exercise is that the QMC-ME results of Sec. III have shown that rapidly upon hole doping the quasiparticle dispersion resembles that of a renormalized noninteracting set of electrons. Then, it is interesting to analyze what would occur with such dispersion as the density *within the qp band* changes (i.e., the density $\langle n \rangle$ shown in Fig. 7 must be considered as the filling of the qp band, rather than the density of the whole system). It is clear from the figure that $(\pi, 0)$ is intrinsically more sensitive to doping than the main diagonal. Actually the results resemble in part those of Marshall *et al.*¹ especially the experimental ARPES dispersion corresponding to slightly underdoped samples of Bi2212 with $T_c = 85$ K, as well as previous experiments for optimally doped samples,⁷ where the qp band crosses the chemical potential between (π, π) and $(\pi, 0)$. This led us to conjecture that the ARPES experiments in the slightly underdoped regime may have observed the hole filling of a ‘‘free like,’’ but narrow, qp band. If this speculation is correct, then it is here predicted that $(\pi, 0)$ will eventually cross the chemical potential when the system becomes overdoped, as Fig. 7 shows. To the best of our knowl-

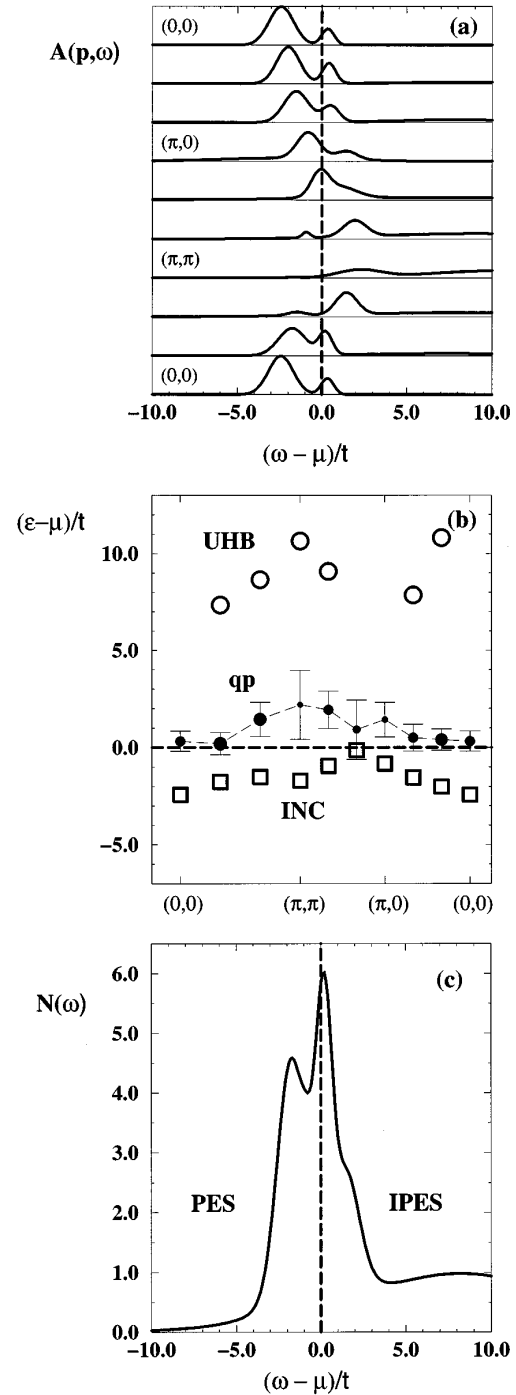


FIG. 4. (a) Spectral functions $A(\mathbf{p}, \omega)$ of the U - t - t' Hubbard model at $U/t = 10$, $t'/t = -0.35$, and $T = t/3$, using QMC-ME techniques on a 6×6 cluster. The density is $\langle n \rangle = 0.78$. From the bottom, the momenta are along the main diagonal from $(0, 0)$ to (π, π) , from there to $(\pi, 0)$, and finally back to $(0, 0)$; (b) energies of the dominant peaks in the spectral functions. The results in the PES region are obtained from a two-Gaussian analysis of the QMC-ME results. The squares correspond to the incoherent part of the spectrum (INC) and its error bars are not shown. The full circles form the quasiparticle (qp) band, and their diameter is proportional to the intensity. The error bars are given by the width at half the height of the Gaussian corresponding to the qp peak at each momenta. The upper Hubbard band is also shown (open circles) without error bars; (c) density of states $N(\omega)$ obtained by summing the $A(\mathbf{p}, \omega)$'s.

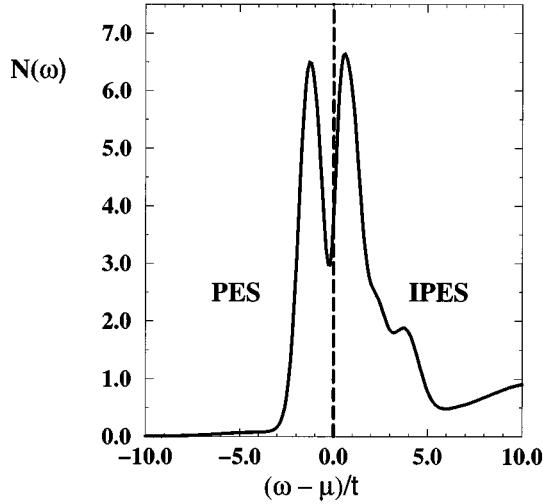


FIG. 5. Density of states $N(\omega)$ corresponding to the U - t - t' Hubbard model at $U/t=10$, $t'/t=-0.35$, and $T=t/3$, using QMC-ME techniques on a 6×6 cluster. The density is $\langle n \rangle = 0.65$.

edge there are no ARPES results in this regime. Experimental work for overdoped cuprates would clarify the issue of whether the “flat bands” found in the optimal regime remain locked near μ or smoothly cross the Fermi energy as the hole doping increases. Our results favor the latter, at least within the resolution of the QMC-ME methods.

Further evidence that $(\pi,0)$ travels across the chemical potential is given in Figs. 8(a) and 8(b). There $A(\mathbf{p},\omega)$ with $\mathbf{p}=(\pi,0)$, taken from Figs. 1(a)–6(a), is shown again adding also results for densities $\langle n \rangle = 0.89$ and 0.65 for completeness. The peak at this momentum belonging to the qp band crosses μ at a density $\langle n \rangle \approx 0.82$. Then, as the hole density grows, a movement up in energy of the $\mathbf{p}=(\pi,0)$ quasiparticle is clearly observed, as in ARPES experiments.³⁵ At a larger hole density, such as quarter-filling, the qp peak, now in the IPES regime, reduces substantially its weight and disappears. At this density the feature associated with the incoherent part of the spectrum at half-filling is now located close to the Fermi energy, contributing to the dispersion that resembles the $U=0$ result [Fig. 6(b)]. The UHB rapidly loses weight moving away from half-filling. Figures 9(a) and 9(b) show similar results but for $\mathbf{p}=(2\pi/3, 2\pi/3)$, which is representative of the behavior along the main diagonal on the 6×6 cluster. The qp associated to this momentum crosses the chemical potential at a smaller hole density ($\langle n \rangle \approx 0.95$).

Summarizing the results of this section, in Fig. 10 three representative qp dispersions obtained with QMC-ME methods (Sec. III) are shown. For the half-filled case the results are accurately known from the self-consistent Born approximation,¹⁰ and $(\pi,0)$ is clearly below the chemical potential, which here is arbitrarily located at the top of the band. Note that the intensity of the qp peak is much weaker near (π,π) than for other momenta at half-filling. For small hole doping densities, such as $\langle n \rangle = 0.84$, a “freelike” but narrow quasiparticle band is observed in QMC simulations (also in studies of the U - t model^{36,25}) and $(\pi,0)$ is now at the Fermi energy. The vicinity of (π,π) is the region affected the most by hole doping due to the reduction of antiferromagnetic correlations. Finally, at lower densities, such as

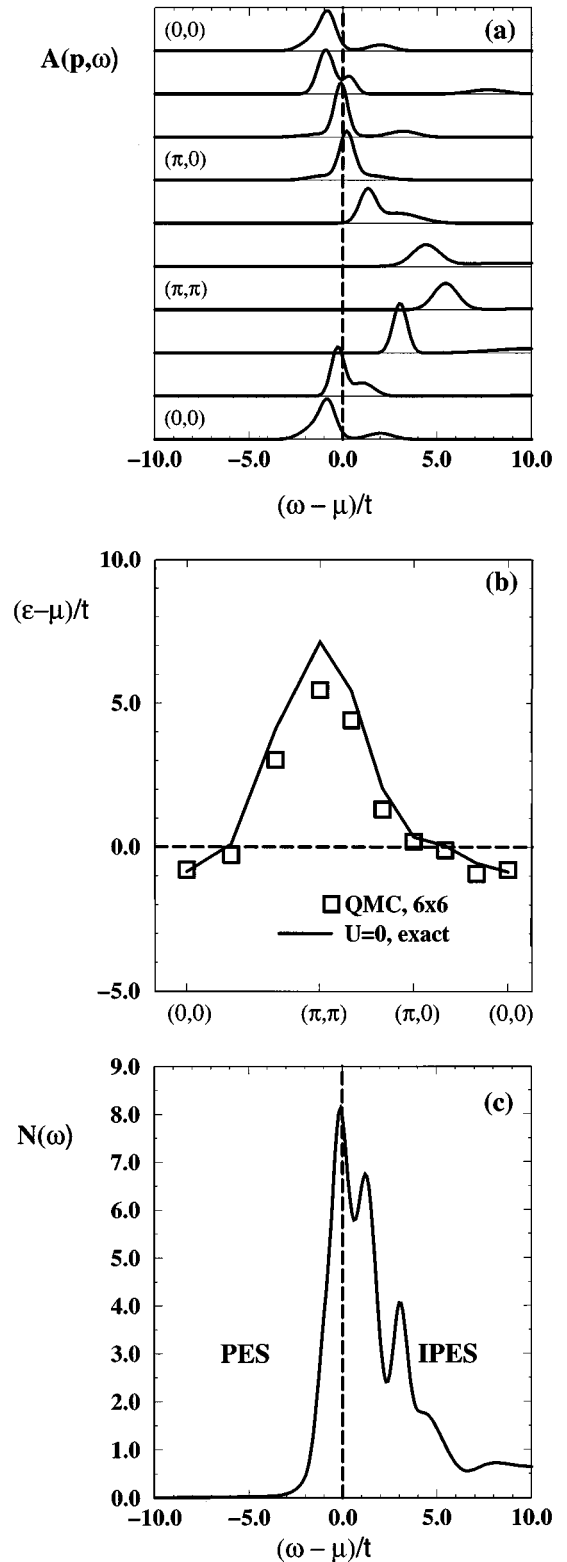


FIG. 6. (a) Spectral functions $A(\mathbf{p},\omega)$ of the U - t - t' Hubbard model at $U/t=10$, $t'/t=-0.35$, and $T=t/3$, using QMC-ME techniques on a 6×6 cluster. The density is $\langle n \rangle = 0.47$. From the bottom, the momenta are along the main diagonal from $(0,0)$ to (π,π) , from there to $(\pi,0)$, and finally back to $(0,0)$; (b) energies of the dominant peaks in the spectral functions. The solid line is the dispersion in the noninteracting limit $U/t=0.0$ on a large cluster; (c) density of states $N(\omega)$ obtained by summing the $A(\mathbf{p},\omega)$'s.

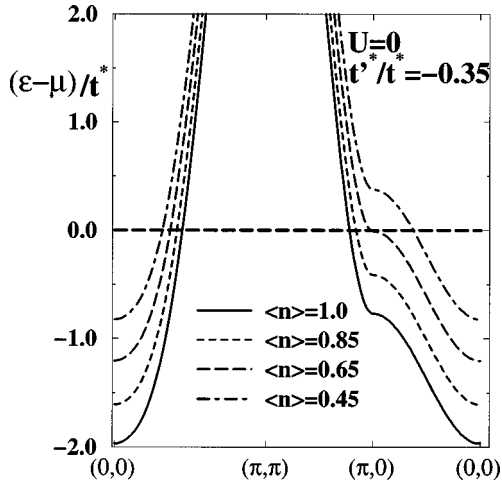


FIG. 7. Density evolution of a noninteracting band, referred to the chemical potential, as its density changes (shown in the figure). For details see the text.

$\langle n \rangle = 0.78$, the chemical potential has crossed the qp band and now $(\pi, 0)$ is above the Fermi energy. We consider that the scenario depicted in Fig. 10 for the density evolution of the qp dispersion can provide a simple qualitative explanation for the ARPES results found experimentally. It predicts that the qp peak at $(\pi, 0)$ will eventually disappear from the ARPES signal into the IPES region, an effect that could be tested experimentally. At densities intermediate between $\langle n \rangle = 1.0$ and 0.84 , the peak at $(\pi, 0)$ should evolve smoothly between these two limits, and thus close to half-filling “pseudogap” features will likely appear in simulations if lower temperatures could be reached. Reducing the temperature below $T = t/3$ is particularly important for the generation of strong spin fluctuations which are crucial to induce the quasiparticle dispersion at half-filling shown in Fig. 10. Note that “shadow” features should actually be present at $\langle n \rangle = 0.84$ but they are too weak to be detected by QMC-ME

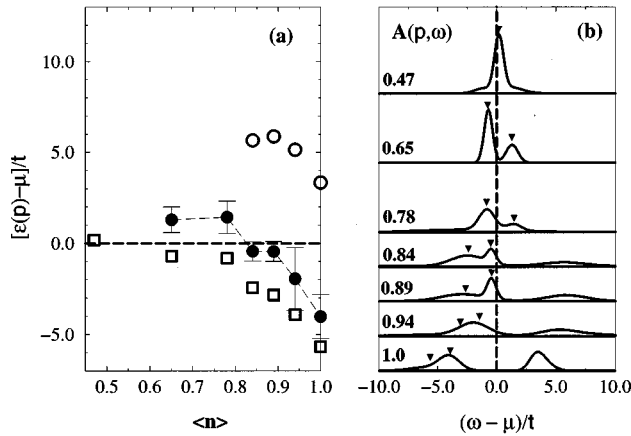


FIG. 8. (a) Energy of the quasiparticle (referred to the chemical potential) in units of t for the U - t - t' Hubbard model using the parameters of Figs. 1–6. The results here correspond to momentum $\mathbf{p} = (\pi, 0)$. The solid circles, squares, and open circles are the qp, INC, and UBH positions for this momentum; (b) quasiparticle spectral function corresponding to momentum $\mathbf{p} = (\pi, 0)$ for several densities $\langle n \rangle$ (indicated). The small triangles show the positions of the dominant peaks in the two-Gaussian analysis of the PES data.

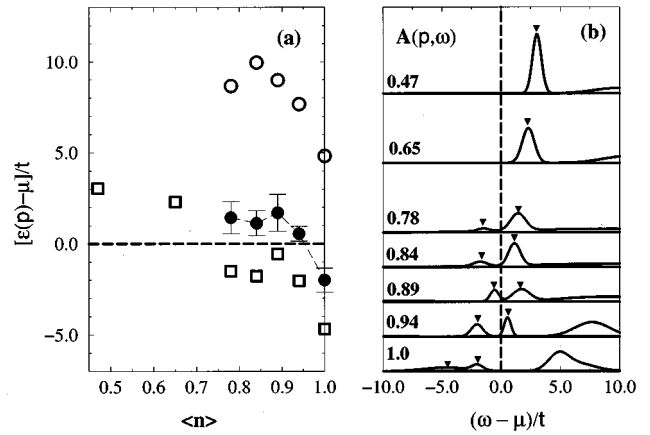


FIG. 9. (a) Energy of the quasiparticle (referred to the chemical potential) in units of t for the U - t - t' Hubbard model using the parameters of Figs. 1–6. The results here correspond to momentum $\mathbf{p} = (2\pi/3, 2\pi/3)$. The solid circles, squares, and open circles are the qp, INC, and UBH positions for this momentum; (b) quasiparticle spectral function corresponding to momentum $\mathbf{p} = (2\pi/3, 2\pi/3)$ for several densities $\langle n \rangle$ (indicated). The small triangles show the positions of the dominant peaks in the two-Gaussian analysis of the PES data.

methods, and probably also by ARPES experiments which have large backgrounds in their signals. Thus, the existence of hole pockets cannot be shown from the current Monte Carlo simulations available.

V. IMPLICATIONS OF QMC RESULTS FOR SOME THEORIES OF HIGH T_c

In this section, the implications of our QMC results for recently proposed scenarios for high- T_c cuprates will be discussed. Two features found in the simulation will be important, namely the “tight-binding” shape of the qp band at finite hole density (although with renormalized parameters) and the crossing of the qp band by μ for densities in the approximate range $0.70 \leq \langle n \rangle \leq 1.0$.

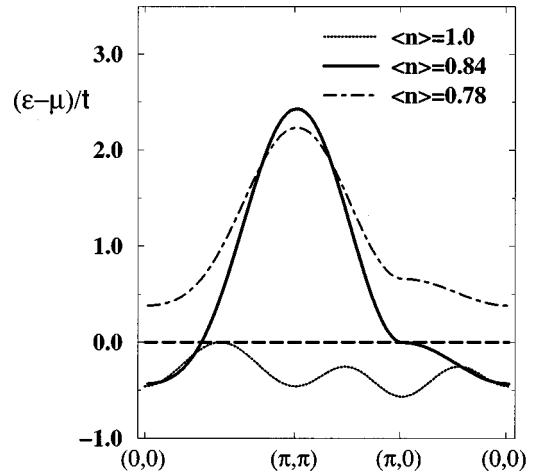


FIG. 10. Best fits of the QMC-ME quasiparticle dispersion corresponding to densities $\langle n \rangle = 0.84$ and $\langle n \rangle = 0.78$. The results at $\langle n \rangle = 1.0$ are taken from Ref. 10 arbitrarily locating the top of the band at the chemical potential.

A. Large peak in the DOS

As explained in the Introduction, the presence of “flat” regions in the experimental normal-state qp dispersion is a remarkable feature of the phenomenology of hole-doped cuprates.⁷ These flat bands are located around momenta $\mathbf{p}=(\pi,0)$ and $(0,\pi)$, and at optimal doping they are ~ 10 meV below the Fermi energy.⁷ Studies of holes in the 2D t - J and Hubbard models at and away from half-filling have suggested that antiferromagnetic correlations may play an important role in the generation of these features.^{32,30,33,36} Our results for the U - t - t' model suggest the presence of flat bands in the regime close to $\langle n \rangle = 0.84$, although care must be taken with the finite resolution of the ME-generated qp peaks. But even if these flat regions were not quantitatively described by one-band electronic models, the intrinsic small bandwidth of the qp band at small hole density could be enough to induce a large peak in the DOS which can be used to enhance the superconducting critical temperature, once a source of hole attraction is identified. This leads to a natural explanation for the existence of an “optimal doping” which in this framework occurs when the peak in the qp band is reached by μ .¹² It is also natural to label as “underdoped” the regime where μ is to the right of the “flat band” peak (i.e., at higher energies), and “overdoped” when it is to the left (i.e., at lower energies).³⁷

Previous analytical calculations¹² assumed the survival of the large DOS obtained at half-filling as the density of holes grows. The results of our simulations (Sec. III) allow us to study the evolution of the DOS with hole density and judge if these ideas are realistic. The presence of a robust qp peak is certainly confirmed by our results, and Figs. 1(b)–4(b) show that as $\langle n \rangle$ decreases from 1, the qp band is crossed by μ as conjectured before.¹² The DOS of the standard t - J and Hubbard models (with $t'=0$) also have a large peak in the DOS, as found in previous numerical simulations. For completeness, here those results are also presented. In Fig. 11(a), $N(\omega)$ for the 2D t - J model obtained with exact diagonalization (ED) techniques is shown at several densities.⁶ At half-filling, a large DOS peak appears at the top of the valence band.³² Note that substantial weight exists at energies far from μ , i.e., the large peak carries only a fraction of the total weight, in agreement with the QMC simulations of Sec. III. In the t - J model, the maximum in the DOS is not strictly located at the top of the valence band but at slightly smaller energies.³² This effect is enhanced by adding t' hopping terms to the t - J Hamiltonian, as shown in the simulation results of Sec. III. As $\langle n \rangle$ decreases, the peak in Fig. 11(a) is now much broader but it remains well defined. At $\langle n \rangle \sim 0.88$, μ is located close to the energy where $N(\omega)$ is maximized. At $\langle n \rangle \sim 0.75$, μ moves to the left of the peak. These results are quantitatively similar to those of our QMC simulations for the U - t - t' model, and also with results for the $t'/t=0.0$ Hubbard model [Fig. 11(b)]. Thus, while accurate extrapolations to the bulk limit are difficult, the simple qualitative picture emerging from these studies, namely that strong correlations generate a qp peak in the DOS which is crossed by μ , seems robust.

As explained before, this qp peak crossing of the DOS is important since once a source of hole attraction exists in the system, a superconducting (SC) gap would open at μ , and

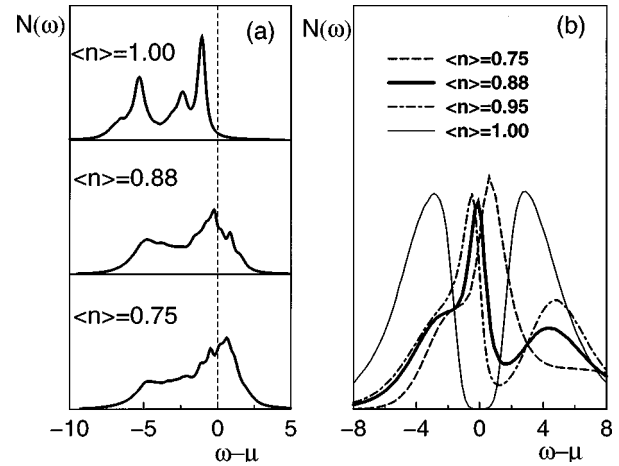


FIG. 11. (a) $N(\omega)$ for the 2D t - J model obtained with exact diagonalization techniques averaging results for clusters with 16 and 18 sites, at $J/t=0.4$ and for the densities indicated. The δ functions were given a width $\eta=0.25t$. Similar results were found at other values of J/t ; (b) $N(\omega)$ for the one-band Hubbard model obtained on a 4×4 cluster using QMC and ME, but without reducing the coefficient of the entropy as in Sec. III. The temperature is $T=t/4$ and $U/t=12$. Densities are indicated.

the resulting T_c could be enhanced due to the large number of states available. The numerical results, both QMC and ED, are thus compatible with scenarios where a large T_c is obtained due to an increase in $N(\mu)$. Since the peak width increases substantially with hole density, strictly speaking the rigid band filling of the half-filled hole dispersion is invalid. However, such an approximation seems to have captured part of the qualitative physics of the problem, since the DOS peak is not washed out by a finite hole density.

In the cases discussed here, i.e., the U - t - t' and t - J models, calculations of the spin-spin correlations show that ξ_{AF} is approximately a couple of lattice spacings when μ is located near the DOS peak, becoming smaller as the overdoped regime is reached. Thus, a nonzero ξ_{AF} and μ near a large DOS peak are *correlated* features. It is in this respect that scenarios where AF correlations produce a large DOS that enhances T_c (Ref. 12) differ from vH theories where divergences in the DOS are caused by band effects already present before interactions are switch on.¹⁶

While the existence of a robust peak in the DOS is in good agreement with ARPES data,⁷ it is in apparent disagreement with specific heat studies for YBCO.³⁸ The lack of \mathbf{p} resolution in the specific-heat measurements may solve this puzzle. Actually, angle-integrated PES results for Bi2212 do not show the sharp flat features found in ARPES for the same material.^{39,40} Similar effects may affect the specific-heat data which should be reanalyzed to search for DOS large peaks.

B. Kondo resonances vs AF-induced quasiparticle

Previous QMC-ME studies of the Hubbard model for $t'/t=0.0$ (Refs. 36, 41 and 18) reported results qualitatively similar to those shown in Fig. 11(b), where the DOS obtained on a 4×4 cluster is presented for the one-band Hubbard model at $U/t=12$, and $T=t/4$. The ME technique used

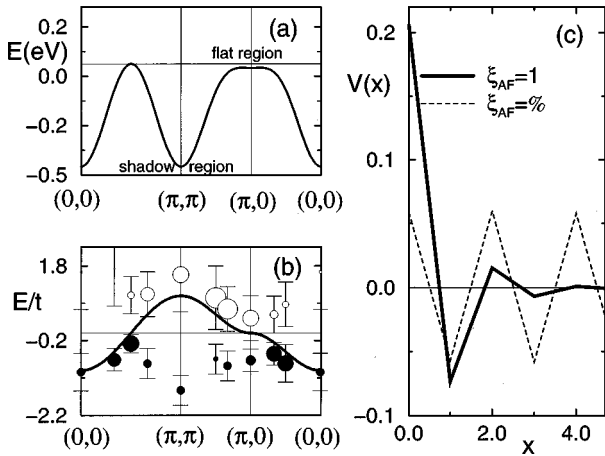


FIG. 12. (a) qp energy vs momentum obtained at half-filling using the t - t' - J (from Refs. 32 and 12). The result shown, which we call $\epsilon_{\text{AF}}(\mathbf{p})$, is a good fit of Monte Carlo data on a 12×12 cluster at $J/t = 0.4$; (b) qp dispersion vs momentum at $\langle n \rangle = 0.87$ and $J/t = 0.4$ using exact diagonalization of 16- and 18-site clusters for the t - J model (from Ref. 25). The open (full) circles are IPES (PES) results. Their size is proportional to the peak intensity. The solid line is the fit $\epsilon_{\text{NN}}(\mathbf{p})$ described in the text; (c) $V(x)$ along the x -axis after Fourier transforming the smeared potential $V(\mathbf{p}) = \delta(\mathbf{p} - \mathbf{Q})$ (see text). ξ_{AF} is given in lattice units.

in Fig. 11(b) is the same as in those previous simulations, and it does not have the resolution of the present ME variation discussed in Sec. III. The crossing of a peak in the DOS by μ is clearly observed in these ME simulations but at half-filling there are no qp peaks. Figure 11(b) can thus be naively interpreted as the ‘‘generation’’ by doping of a Kondo-like peak at the top of the valence band which does not exist at $\langle n \rangle = 1$. However, our current results [Fig. 1(c)] actually show that at $\langle n \rangle = 1.0$ a well-defined qp peak is present, as predicted by a variety of studies of the zero temperature t - J model with one hole.^{6,25} Also experimentally in the cuprates it has been already established³⁹ that the states observed in PES upon doping are already present in the insulator and are *not* Kondo resonances. Thus, Figs. 1(b)–4(b) provide evidence that the qp features observed at $\langle n \rangle < 1$ are smoothly connected to peaks already present at half-filling. Similar conclusions have also been obtained in geometries other than the 2D square lattice, such as a t - J ladder.^{31,42}

C. $d_{x^2-y^2}$ in the Hubbard model

The results of Figs. 1(b)–6(b) show that the qp band is very sensitive to doping, at least at the temperatures and couplings used in this QMC-ME study. In particular a few percent hole doping is enough to transform the half-filling dispersion, containing the extra symmetry induced by long-range AF order, into a tight-binding-like dispersion although with a small hopping amplitude. These results are similar to others previously published in the literature. For example, in Figs. 12(a) and 12(b) the qp dispersion at $\langle n \rangle = 1$ and at $\langle n \rangle \sim 0.87$ for the t - J model is reproduced from Ref. 25 (for Hubbard model results, see Refs. 36 and 43). Upon doping, vestiges of the flat regions remain, inducing a large peak in the DOS (see Fig. 11). However, the region around $\mathbf{p} = (\pi, \pi)$ has changed substantially, i.e., the AF shadow

region observed at $\langle n \rangle = 1$ reduced its intensity and considerable weight was transferred to the IPES region. The qp dispersion at $\langle n \rangle \sim 0.87$ of the t - J model can also be fitted by a tight-binding nearest-neighbor (NN) dispersion with a small effective hopping likely associated with J . Then, both previous literature results and the present simulations agree on the qualitative aspects of the evolution with doping of $A(\mathbf{p}, \omega)$.

The changes in the qp dispersion with hole doping can be interpreted in two ways. First, note that $A(\mathbf{p}, \omega)$ is influenced by matrix elements of *bare* fermionic operators connecting states with N and $N \pm 1$ particles. This is important when the qp weight is small, i.e., when the state $c_{\mathbf{p}\sigma} |g.s.\rangle_N$ does not have a large overlap with the ground state of the $N-1$ particles subspace $|g.s.\rangle_{N-1}$ ($|g.s.\rangle_N$ being the ground state with N particles). If the hole excitation is instead created by a new operator $\gamma_{\mathbf{p}\sigma}$ that incorporates the dressing of the hole by spin fluctuations, then $\gamma_{\mathbf{p}\sigma} |g.s.\rangle_N$ may now have a large overlap with $|g.s.\rangle_{N-1}$.^{44,45} In other words, if the dressed hole state resembles an extended spin polaron, then the physics deduced from PES studies, which rely on the sudden removal of a bare electron from the system, may be misleading. To the extent that spin polarons remain well defined at finite density, the use of $\gamma_{\mathbf{p}\sigma}$ will induce spectral weight rearrangements between the PES and IPES regions, and the results at small hole density could resemble those at half-filling after such spectral weight redistribution takes place. If this idea were correct, then the study of superconductivity and transport, both regulated by *dressed* quasiparticles, could indeed be handled by filling a rigid band given by $\epsilon_{\text{AF}}(\mathbf{p})$. It is likely that this idea will work in the underdoped regime where ξ_{AF} is robust, and results for 2D clusters⁴⁵ and ladders⁴⁶ already support these claims. Note that the fact that the bandwidth at finite hole density remains much smaller than $8t$ shows that strong correlations still play an important role in the dispersion. It is interesting to remark that strictly speaking a rigid band filling of the dispersion shown in Fig. 12(a) can generate IPES weight near $(\pi/2, \pi/2)$, but never at (π, π) . Such IPES (π, π) states exist at finite hole density as shown in Fig. 12(b). Thus, the rigid band filling will always be an approximation and it can never be exact. Nevertheless, it is possible that large weight changes introduced by the use of quasiparticle operators can produce a spectral function that approximates well Fig. 12(a), i.e., having a tiny weight at the IPES (π, π) states. More work is needed to clarify if dressed operators are a useful concept in the context of lightly doped antiferromagnets.

An alternative is that the difference between Figs. 12(a) and 12(b) for the t - J model and Figs. 1(b) and 2(b) for the U - t - t' model correspond to an intrinsic change in the qp dispersion as ξ_{AF} decreases. This is the less favorable case for the real-space pairing approaches¹² which are constructed at half-filling, and thus we should analyze this possibility in detail here. For this purpose, we have applied the standard BCS formalism to an effective model with a low density of quasiparticles having a dispersion $\epsilon_{\text{NN}}(\mathbf{p})/eV = -0.2(\cos p_x + \cos p_y)$ (assuming $t = 0.4$ eV), which roughly reproduces the dominant features of Fig. 12(b). [The reader should not confuse this dispersion with that of free particles whose bandwidth is four times larger. A large amount of incoherent weight is still observable at the density of Fig.

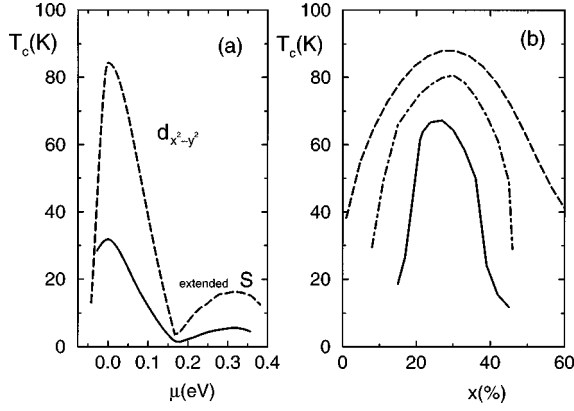


FIG. 13. (a) T_c vs μ obtained with the BCS gap equation, with $\mu=0$ as the chemical potential corresponding to the saddle point. The dashed line corresponds to results using $\epsilon_{AF}(\mathbf{p})$, and the solid line to $\epsilon_{NN}(\mathbf{p})$. Interpolations between these two-extreme cases can be easily constructed using two-band models with weights regulated by Z factors (actually we calculated T_c using a two-pole Green's function in the gap equation and the result smoothly interpolated between those shown in the figure). Note the presence of both $d_{x^2-y^2}$ -wave and extended s -wave SC; (b) T_c for d -wave SC vs the percentage x of filling of the qp band (i.e., *not* of the full system). The dashed line is the same as in (a). The solid line corresponds to the BCS gap equation result making zero the weight Z_p of states in the qp dispersion that are at energies from the saddle point larger than 2.5% of the total bandwidth (i.e., basically including states only in a window of energy ~ 125 K around the flat regions). The dot-dashed line is the same but using a window of ~ 250 K around the flat regions.

12(b) although it is not shown explicitly. The same occurs in Fig. 2(b) for the U - t - t' model.] As described before, to study T_c we should include a NN attraction induced by AF between these quasiparticles. While naively it may seem dubious to use the same interaction both at and away from half-filling, the hole-hole potential should not be much affected at distances shorter than ξ_{AF} . This can be illustrated by a real-space analysis [Fig. 12(c)] of a smeared δ -function potential of AF origin $V(\mathbf{q}) = \xi_{AF} / [1 + \xi_{AF}^2 (\mathbf{q} - \mathbf{Q})^2]$, where the lattice spacing is set to 1, and $\mathbf{Q} = (\pi, \pi)$. Figure 12(c) shows that the NN potential ($x=1$) does not change noticeably as ξ_{AF} is reduced, while $V(x>1)$ is rapidly suppressed. Then, using the same NN form of the potential for many densities should not be a bad approximation.⁴⁷

To analyze the stability of previous calculations let us then use the tight-binding dispersion $\epsilon_{NN}(\mathbf{p})$ obtained from the numerical analysis in the BCS gap equation. Solving numerically the gap equation, T_c is shown in Fig. 13(a). As reported before,¹² superconductivity at $T_c \sim 80$ –100 K in the $d_{x^2-y^2}$ channel appears naturally if the hole dispersion $\epsilon_{AF}(\mathbf{p})$ at half-filling is used. Nevertheless, if instead $\epsilon_{NN}(\mathbf{p})$ is used, the vestiges of the flat bands present in this narrow dispersion produce $T_c \sim 30$ K which is still large.⁴⁸ The critical temperature may be further enhanced if attraction at distances larger than one lattice spacing are considered, as observed in a recent self-consistent Eliashberg-Ansatz calculation within the fluctuation exchange approximation.⁴⁸ Even more remarkable is the fact that the $d_{x^2-y^2}$ character of the SC state is maintained. This result can be understood

noticing that a combination of $\epsilon_{NN}(\mathbf{p})$ with an attractive NN potential effectively locates the Hamiltonian in the family of “ t - U - V ” models with U repulsive and V attractive, where it is known that for a “half-filled” electronic band the dominant SC state is $d_{x^2-y^2}$ -wave.⁴⁹ In other words, when μ is at the flat region of the $\epsilon_{NN}(\mathbf{p})$ dispersion it approximately corresponds to an effective “half-filled” qp band resembling a free electron dispersion (but with smaller bandwidth), leading to a $d_{x^2-y^2}$ -wave SC state [Fig. 13(a)]. Then, even if the qp dispersion changes substantially with doping near the $\mathbf{Q} = (\pi, \pi)$ point, such an effect does *not* seem to alter the main qualitative features found in previous studies.¹² This is a remarkable result, and it is caused by the rapid depopulation of the qp band as the hole density grows. Then, while $\langle n \rangle$ governs the actual global density of the system, there is a subtle *hidden* density (i.e., the population of the qp band) that may influence considerably on the physics of the problem. At $\langle n \rangle = 0.78$ and for the U - t - t' model, this qp band is nearly empty while globally the system is still close to half-filling. While the use of $\epsilon_{AF}(\mathbf{p})$ or $\epsilon_{NN}(\mathbf{p})$ is certainly a rough approximation, the existence of a robust T_c and d -wave superconductivity in both cases suggests that similar results would be obtained using more realistic models for the hole pairing interaction.

D. Influence of shadow bands on SC

The present analysis also shows that the AF “shadow” regions of the half-filling hole dispersion $\epsilon_{AF}(\mathbf{p})$ are not crucial for the success of the real-space approach. Using $\epsilon_{NN}(\mathbf{p})$, which does not contain weight in PES near (π, π) , T_c is still robust and the d -wave state remains stable, as shown in the previous subsection. To establish this result more clearly, we analyzed T_c using $\epsilon_{AF}(\mathbf{p})$ but modulating the contribution of each momentum with a \mathbf{p} -dependent weight Z_p in the one-particle Green's function. We considered the special case where Z_p is zero away from a window of total width W centered at the saddle point, which is located in the flat bands region. Inside the window W , the weight is maximum, i.e., $Z_p = 1$. Such a calculation also addresses indirectly possible concerns associated with widths $\sim [\epsilon_{AF}(\mathbf{p}) - \epsilon_F]^2$ that qp peaks would acquire away from half-filling in standard Fermi liquids (ϵ_F is the Fermi energy). Results are shown in Fig. 13(b), for d -wave SC. Note that even in the case where W is as small as just 5% of the total bandwidth (itself already small of order $2J$), T_c remains robust and close to 70 K. Then, it is clear that the dominant contribution to T_c comes from the flat regions and the shape of the qp dispersion away from them has a secondary importance for the success of the real-space approach. However, it is important to remark that the calculation described in this section showing that shadow features are not very important for the actual value of T_c does not mean that AF correlations can be neglected. On the contrary, the whole antiferromagnetic van Hove scenario¹² and other similar approaches are based on the notion that pairing is caused by spin fluctuations. In addition, in Ref. 50 it is argued that the doping dependence of the AF correlation, which generates the shadow features, changes even more the role of spin fluctuations for superconductivity. For instance, lifetime effects of the quasiparticles can lead to important consequences for

Cooper pair formation⁵⁰ beyond the scope of the theory presented in this paper. More work is needed to clarify all these important aspects of the problem.

E. SC in the overdoped regime

Finally, novel predictions obtained in the regime where the qp band is almost fully crossed by μ (as observed in Sec. III for $\langle n \rangle$ between 0.78 and 0.66) are discussed here. From the point of view of the qp band this regime is “dilute” but, again, this should not be confused with the bottom of the whole spectrum since a large amount of weight remains in the incoherent part of $A(\mathbf{p}, \omega)$. At this density a standard BCS gap equation analysis applied to a qp dispersion either constructed at half-filling, as in Ref. 12, or phenomenologically obtained from our data [$\epsilon_{\text{NN}}(\mathbf{p})$], and supplemented by nearest-neighbor attraction induced by antiferromagnetism, shows that extended s -wave SC dominates over $d_{x^2-y^2}$ -wave SC. This corresponds to the “overdoped” regime [Fig. 13(a)], i.e., to an overall density in the vicinity of $\langle n \rangle \sim 0.70$.⁵¹ This change in the symmetry of the SC state can be understood recalling once again that the tight-binding dispersion of the qp, even including renormalized amplitudes, supplemented by a NN attraction, formally corresponds to an effective “ t - U - V ” model. It is well known that in this model the SC state symmetry changes from d to s wave as the density is reduced away from half-filling to a nearly empty system.^{49,52} Actually the bound state of two particles on an otherwise empty lattice with a NN tight-binding dispersion and NN attraction is s wave. To the extent that the AF or NN dispersions survive up to $\sim 25\%$ hole doping, as suggested by the numerical data of Sec. III as well as previous literature (Ref. 25 and references therein), scenarios based on the real-space interaction of qp’s predict a competition between extended s -wave and $d_{x^2-y^2}$ -wave SC in the *overdoped* regime. Recent calculations based on the analysis of the low electronic density $\langle n \rangle \ll 1$ limit of the t - J model led to analogous conclusions.⁵³ Our approach is based on a very different formalism but it arrives at similar results, and, thus, a crossover from d - to s -wave dominated superconductivity in overdoped cuprates could occur. Indeed recent ARPES data for overdoped Bi2212 have been interpreted as corresponding to a mixing of s - and d -wave

states.⁵⁴ More work should be devoted to this potential competition between d - and s -wave for overdoped cuprates.

VI. SUMMARY

In this paper the results of an extensive numerical study of the U - t - t' one-band Hubbard model with $t'/t = -0.35$ have been presented. The regime of strong coupling $U/t = 10$ was analyzed. These parameters are fixed to reproduce ARPES data for the AF insulator. With maximum entropy techniques, the spectral function $A(\mathbf{p}, \omega)$ was studied for several electronic densities. It was observed that as the hole density grows away from half-filling, the quasiparticle band acquires “noninteracting” features although with bandwidths substantially smaller than for the $U = 0$ limit. As the hole density increases, the qp peak at $(\pi, 0)$ rapidly changes its position relatively to the Fermi energy, in qualitative agreement with recent ARPES experiments.^{1,2} In the overdoped regime, it is predicted that the flat bands should be crossed by the chemical potential and thus they should no longer be observed in ARPES studies. The present results also have implications for some theories of high T_c . The narrow qp band produces a large peak in the DOS induced by strong correlations, which survives the presence of hole doping, and it can be used to boost T_c once a source of hole attraction is found. It is remarkable that both with the hole dispersion found at half-filling or the one observed using QMC-ME at, e.g., $\langle n \rangle = 0.84$, superconductivity in the $d_{x^2-y^2}$ channel dominates. This result gives support to real-space pairing theories of high T_c ,¹² showing that the main ideas of the scenario are stable upon the introduction of a finite hole density. The large DOS peak is crossed by the chemical potential as $\langle n \rangle$ is reduced. In the overdoped regime, i.e., when the qp band is almost empty, a possible competition between extended- s and $d_{x^2-y^2}$ SC was discussed.

ACKNOWLEDGMENTS

We thank A. Sandvik, M. Onellion, D. Dessau, J. C. Campuzano, and Z. X. Shen for useful discussions. D.D. is supported by Grant No. ONR-N00014-94-1-1031. A.M. and E.D. are supported by Grant No. NSF-DMR-9520776. Additional support by the National High Magnetic Field Lab and Martech is acknowledged.

¹D. S. Marshall *et al.*, Phys. Rev. Lett. **76**, 4841 (1996).

²H. Ding *et al.*, Nature (London) **382**, 51 (1996).

³S. LaRosa, I. Vobornik, H. Berger, G. Margaritondo, C. Kendziora, R.J. Kelley, and M. Onellion (unpublished).

⁴B. O. Wells, Z.-X. Shen, A. Matsuura, D. M. King, M. A. Kastner, M. Greven, and R. J. Birgeneau, Jr., Phys. Rev. Lett. **74**, 964 (1995).

⁵M. Grioni, H. Berger, S. LaRosa, I. Vobornik, F. Zwick, G. Margaritondo, R. J. Kelley, J. Ma, and M. Onellion, Physica B (to be published).

⁶For a review see E. Dagotto, Rev. Mod. Phys. **66**, 763 (1994).

⁷D. S. Dessau *et al.*, Phys. Rev. Lett. **71**, 2781 (1993); K. Gofron *et al.*, *ibid.* **73**, 3302 (1994); J. Ma *et al.*, Phys. Rev. B **51**, 3832 (1995).

⁸D. Doniach *et al.*, Phys. Rev. B **41**, 6668 (1990); V. J. Emery *et al.*, Nature (London) **374**, 434 (1995), and references therein.

⁹Note that recent ARPES results found no evidence of small hole pockets in underdoped Bi2212 even in samples with a critical temperature as small as 15 K. Thus, the presence of pocket features in ARPES is still under much discussion [see H. Ding, M. R. Norman, T. Yokoya, T. Takeuchi, M. Randeria, J. C. Campuzano, T. Takahashi, T. Mochiku and K. Kadowaki, Phys. Rev. Lett. **78**, 2628 (1997)].

¹⁰A. Nazarenko, K. Vos, S. Haas, E. Dagotto, and R. Gooding, Phys. Rev. B **51**, 8676 (1995).

¹¹O. Starykh, O. de Alcantara Bonfim, and G. Reiter, Phys. Rev. B **52**, 12 534 (1995); B. Kyung and R. Ferrell *ibid.* **54**, 10125 (1996); T. Xiang and J. M. Wheatley, *ibid.* **54**, R12 653 (1996);

- T. K. Lee and C. T. Shih, *ibid.* **55**, 5983 (1997); V. I. Belinicher, A. L. Chernyshev, and V. A. Shubin, *ibid.* **54**, 14 914 (1997); P. W. Leung, B. O. Wells, and R. J. Gooding (unpublished).
- ¹²E. Dagotto, A. Nazarenko, and A. Moreo, Phys. Rev. Lett. **74**, 310 (1995).
- ¹³D. J. Scalapino, Phys. Rep. **250**, 331 (1995).
- ¹⁴A. Kampf and J. R. Schrieffer, Phys. Rev. B **41**, 6399 (1990); **42**, 7967 (1990).
- ¹⁵Q. P. Li, B. E. C. Koltenbah, and R. J. Joynt, Phys. Rev. B **48**, 437 (1993).
- ¹⁶C. C. Tsuei *et al.*, Phys. Rev. Lett. **65**, 2724 (1990); R. S. Markiewicz, J. Phys., Condens. Matter. **2**, 6223 (1990); A. A. Abrikosov *et al.*, Physica C **214**, 73 (1993).
- ¹⁷P. Aebi *et al.*, Phys. Rev. Lett. **72**, 2757 (1994).
- ¹⁸S. Haas *et al.*, Phys. Rev. Lett. **74**, 4281 (1995).
- ¹⁹S. LaRosa, R. J. Kelley, C. Kendziora, G. Margaritondo, M. Onellion, and A. Chubukov (unpublished).
- ²⁰R. Blankenbecler, D. J. Scalapino, and R. Sugar, Phys. Rev. D **24**, 2278 (1981).
- ²¹R. N. Silver, D. S. Sivia, and J. E. Gubernatis, Phys. Rev. B **41**, 2380 (1990); J. E. Gubernatis *et al.*, *ibid.* **44**, 6011 (1991).
- ²²R. Preuss *et al.*, Phys. Rev. Lett. **73**, 732 (1994).
- ²³S. R. White, Phys. Rev. B **44**, 4670 (1991); N. Bulut, D. J. Scalapino, and S. R. White, *ibid.* **50**, 7215 (1994).
- ²⁴R. Preuss, W. Hanke, and W. von der Linden, Phys. Rev. Lett. **75**, 1344 (1995).
- ²⁵A. Moreo *et al.*, Phys. Rev. B **51**, 12 045 (1995).
- ²⁶D. Duffy and A. Moreo, Phys. Rev. B **52**, 15 607 (1995).
- ²⁷Care is needed when using this technique, since spurious features may arise in the spectral function. By monitoring the ME result for $A(\mathbf{p}, \omega)$ while systematically reducing α , we were able to stop the ME analysis before spurious features arose. Furthermore, to check the convergence of the spectral function, several default models were used, and we found that all gave very similar results. For a complete discussion of the influence of the α parameter see Ref. 21.
- ²⁸Note that the sign problem is most severe near optimal doping. Furthermore, the sign problem increases with coupling strength and with the magnitude of t' .
- ²⁹A. Chubukov, Phys. Rev. B **52**, R3840 (1995); J. Schmalian, M. Langer, S. Grabowski, and K. H. Bennemann, *ibid.* **54**, 4336 (1996).
- ³⁰M. Langer, J. Schmalian, S. Grabowski, and K. H. Bennemann, Phys. Rev. Lett. **75**, 4508 (1995).
- ³¹S. Haas and E. Dagotto, Phys. Rev. B **54**, R3718 (1996).
- ³²E. Dagotto, A. Nazarenko, and M. Boninsegni, Phys. Rev. Lett. **73**, 728 (1994).
- ³³R. Putz, R. Preuss, A. Muramatsu, and W. Hanke, Phys. Rev. B **53**, 5133 (1996).
- ³⁴Similar results have been recently obtained by M. Ulmke, R. T. Scalettar, A. Nazarenko, and E. Dagotto, Phys. Rev. B **54**, 16 523 (1996), in the context of the 3D one-band Hubbard model.
- ³⁵See R. Eder, Y. Ohta, and G. A. Sawatzky, Phys. Rev. B **55**, R3414 (1997), where exact diagonalization techniques applied to the t - t' - t'' - J model give results similar to ours regarding the behavior of the qp band near $(\pi, 0)$ as the hole density grows away from half-filling.
- ³⁶N. Bulut, D. J. Scalapino, and S. R. White, Phys. Rev. B **50**, 7215 (1994).
- ³⁷Note that implicitly we are here assuming that the $N(\omega)$ obtained by adding the numerically calculated $A(\mathbf{p}, \omega)$'s can be related with the density of states that would appear in a BCS gap equation. The difference resides in the matrix elements that modulate the intensity in photoemission calculations.
- ³⁸J. W. Loram *et al.*, Phys. Rev. Lett. **71**, 1740 (1993).
- ³⁹A. Fujimori *et al.*, Phys. Rev. B **39**, 2255 (1989); **40**, 7303 (1990).
- ⁴⁰J. M. Imer *et al.*, Phys. Rev. Lett. **62**, 336 (1989).
- ⁴¹N. Bulut, D. J. Scalapino, and S. R. White, Phys. Rev. Lett. **72**, 705 (1994).
- ⁴²M. Troyer, H. Tsunetsugu, and T. M. Rice, Phys. Rev. B **53**, 251 (1996). Note that pairing on ladders may exist [see E. Dagotto and T. M. Rice, Science **271**, 618 (1996) and references therein]. Thus, a gap may open at μ once couplings and lattice sizes are reached where pairing effects are important. We have observed such effects in our studies, but we also found that at $\langle n \rangle = 1$ the DOS has a sharp peak. Then, the numerically observed ladder DOS peak cannot be attributed exclusively to a BCS redistribution of spectral weight upon doping.
- ⁴³E. Dagotto, F. Ortolani, and D. Scalapino, Phys. Rev. B **46**, 3183 (1992).
- ⁴⁴E. Dagotto and J. R. Schrieffer, Phys. Rev. B **43**, 8705 (1991).
- ⁴⁵R. Eder and Y. Ohta, Phys. Rev. B **50**, 10 043 (1994).
- ⁴⁶J. Riera and E. Dagotto, Phys. Rev. B **55**, 14 543 (1997).
- ⁴⁷Note also that the local character of the real-space potential does not imply small Cooper pairs. Their size can be regulated using both its range and intensity.
- ⁴⁸S. Grabowski *et al.*, Europhys. Lett. **34**, 219 (1996).
- ⁴⁹R. Micnas *et al.*, Rev. Mod. Phys. **62**, 113 (1990).
- ⁵⁰See, for example, J. R. Schrieffer, J. Low Temp. Phys. **99**, 397 (1995); S. Grabowski *et al.* (Ref. 48); A. V. Chubukov *et al.* (unpublished), and references therein.
- ⁵¹This is not in contradiction with the observation of d -wave SC at quarter-filling reported in E. Dagotto and J. Riera, Phys. Rev. Lett. **70**, 682 (1993), since these results were obtained at large J/t .
- ⁵²E. Dagotto *et al.*, Phys. Rev. B **49**, 3548 (1994).
- ⁵³B. E. C. Koltenbah and R. Joynt (unpublished). See also D. van der Marel, Phys. Rev. B **51**, 1147 (1995).
- ⁵⁴J. Ma, C. Quitmann, R. J. Kelley, H. Berger, G. Margaritondo, and M. Onellion, Science **267**, 862 (1995).